

Vibration-based crack prediction on a beam model using hybrid butterfly optimization algorithm with artificial neural network

Abdelwahhab KHATIR^a, Roberto CAPOZUCCA^a, Samir KHATIR^{b*}, Erica MAGAGNINI^a

^a Structural Section DICEA, Polytechnic University of Marche, Ancona 60131, Italy

^b Faculty of Civil Engineering, Ho Chi Minh City Open University, Ho Chi Minh City 700000, Vietnam

*Corresponding author. E-mail: Khatir_samir@hotmail.fr

© Higher Education Press 2022

ABSTRACT Vibration-based damage detection methods have become widely used because of their advantages over traditional methods. This paper presents a new approach to identify the crack depth in steel beam structures based on vibration analysis using the Finite Element Method (FEM) and Artificial Neural Network (ANN) combined with Butterfly Optimization Algorithm (BOA). ANN is quite successful in such identification issues, but it has some limitations, such as reduction of error after system training is complete, which means the output does not provide optimal results. This paper improves ANN training after introducing BOA as a hybrid model (BOA-ANN). Natural frequencies are used as input parameters and crack depth as output. The data are collected from improved FEM using simulation tools (ABAQUS) based on different crack depths and locations as the first stage. Next, data are collected from experimental analysis of cracked beams based on different crack depths and locations to test the reliability of the presented technique. The proposed approach, compared to other methods, can predict crack depth with improved accuracy.

KEYWORDS damage prediction, ANN, BOA, FEM, experimental modal analysis

1 Introduction

Structural health monitoring (SHM) has been used to assess civil engineering structures when subjected to a sudden loading. Hence damage prediction and detection have been a subject of focus in recent years. Cracks are one of the most prevalent types of structural damage, and they are created by the repeated stress of a structure. The presence of cracks can cause a structural component to collapse prematurely, posing a risk of incident, injury, and financial loss. As a result, if damage is recognized early in their development, a system's overall safety and durability may be assured. Vibrational analysis of the structure is one of the damage detection approaches that has been developed over time. The general concept of vibrational analysis is that when a crack or damage exists, the modal frequencies of the object vary from their

original value [1,2]. The Artificial Neural Network (ANN) is an essential component of Machine Learning, and it is a type of computational structure that is modeled on the human neural system. As a result, if enough data is supplied to the neural network, it can efficiently anticipate the position of cracks in a damaged beam. Kumar et al. [3] trained an ANN based on frequency ratio values, considering cracks at different locations in a cantilever beam and then estimating the damage location. It was found that the ANN could locate cracks with high accuracy and with low error. Several studies applied the same approach to steel plates, pipes, and bridges [4–9]. Hence the results proved the efficiency of the application. Maity and Saha [10] applied a neural network, using strain and displacement, to understand the behavior of an intact beam as well as a beam that had been damaged in various ways. Their results showed that the network performance improved when the strain was used as an input pattern instead of displacement. The vibration-

based damage detection algorithms have attracted the research community's interest, and a variety of time-domain techniques and input-output modal identification approaches have been used [11,12]. In Ref. [13], the authors employed natural frequencies as input for damage diagnosis using an optimization approach. Lee et al. [14] investigated the use of ANN-based structural damage detection (SDD) in bridges. The damage was presented as flaws and modeled using FEM to extract the data. The ANN-based SDD approach considered the modal features as well as the modeling errors of the baseline FE model from which the training patterns were generated. Anitescu et al. [15] applied ANN to solve boundary value problems using a collocation method. The method used only scattered sets of points for the training and evaluation sets, so there was no mesh. Results for the chosen parameters were shown to be accurate. The application of Deep Neural Network (DNN) has been investigated [16–19] to analyze boundary value issues and Kirchhoff plate bending and vibration analysis. The authors avoided a classical discretization and considered DNNs to be function approximation machines, combining experiments and simulations within one framework. Nanthakumar et al. [20] created an approach based on inverse analysis to predict the inclusion of interfaces in a piezoelectric structure. The displacement and potential electric fields were calculated for each iteration using the extended finite element method (XFEM) to determine the responses for varying inclusion interfaces due to its mesh independence. This proposed methodology could identify defects such as cracks and impurities with low stiffness and permittivity compared with the actual piezoelectric material. The technique suggested here has a significant benefit in that it uses various tools and concepts produced by a very active community.

Arora and Singh [21] proposed a new optimization technique, namely the Butterfly Optimization Algorithm (BOA). They conducted numerous studies on BOA and later, Arora and Singh [22] suggested an enhanced butterfly optimization approach using ten chaotic maps to solve three engineering optimisation problems. They also developed a hybrid optimization technique that combined BOA with the Artificial Bee Colony (ABC) algorithm [23]. Several researchers have demonstrated the effectiveness of artificial intelligence (AI) algorithms such as Genetic Algorithms (GA) in solving minimization problems [24,25]. GA robust global optimization algorithms have been effectively employed to address a comprehensive class of structural problems in the engineering sector. In addition, GA is a quite interesting method compared to conventional optimization methods because it does not require a search throughout the whole solution space [26–28]. Lai and Zhang [29] introduced a new hybrid method that combined Particle Swarm Optimization (PSO) and GA and the results of 23 benchmark problems.

Furthermore, several alternative approaches based on damage identification have been widely utilized to determine the damage identification and predict the true structures' behavior. Truss structures and thin plates were analysed for damage identification using Bat algorithm [30,31]. Ghannadi and Kourehli [32] proposed a structural damage identification method using the Moth-Flame Optimization algorithm MFO. Moezi et al. [33] applied a modified Cuckoo Search (CS) algorithm to determine crack depth and location in a cantilever beam. Also, Kim and Stubbs [34] presented a technique based on modal sensitivity that can detect a crack position in a thin cracked beam. Huang et al. [35] suggested the CS algorithm could be combined with PSO to predict structural damages under temperature variation. Also, Baghmisheh et al. [36] combined PSO with Nelder-Mead, using NM-PSO to determine edge-crack position and depth in a cantilever beam. This method gave results with high accuracy. Next, the last authors used the GA for cracks detection in beam-like structures in Ref. [37]. In order to improve the ANN training performance, many other researchers also combined ANN with bio-inspired algorithms [38–44]. Chatterjee et al. [45] trained the neural network with PSO for failure prediction of multistoried RC buildings. The suggested ANN-PSO classifier could solve the problem of predicting structural failure of multistoried reinforced concrete structures by detecting the possibility of future structural failure.

This paper considers a combined approach based on ANN and BOA for structural damage identification by discussing a typical benchmark and emphasizes the need for a proper specification of the error function that assesses the differences between experimental data and FE model results. The main objective of this paper is to look into the use of the developed hybrid algorithm BOA-ANN to determine the crack depth in a cracked steel beam by minimizing the cost function and to compare BOA-ANN with existing approaches, GA-ANN and PSO-ANN, to assess its accuracy via both numerical and experimental tests.

2 Optimization method description using BOA and ANN

This section discusses the hybrid strategy for optimizing the parameters of ANN prediction models after combining local and global search algorithms. Thoroughly linked layered feedforward networks are used in ANN prediction models. Each unit in the network, except input units, has a bias.

2.1 Artificial Neural Network

ANN is one of the disciplines of AI that involves automating the learning of an algorithm based on data

collecting. This article uses a supervised learning model to estimate the potential crack depth. In order to predict the size of the damaged part, the regression function is explored. Three layers of nodes, including a hidden layer, input layer, and output layer, were the subject of the ANN model, as presented in Fig. 1.

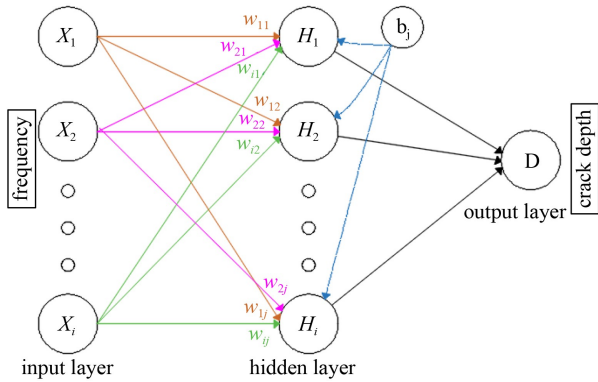


Fig. 1 ANN structure for crack depth identification.

Based on the data chosen from experimental or numerical studies, the number of neurons per layer that can be selected depends on the problems to be analyzed. For more detail, two formulations can be used to study the gathered data from the first phase to the last one.

$$\hat{\Phi}_j = \hat{\Phi} \left(\sum_{i=1}^n w_{ij} f_i + b_i \right), \quad j = (1-m), \quad (1)$$

$$O_j^1 = \frac{1}{1 + e^{-\hat{\Phi}_j}}, \quad (2)$$

where $\hat{\Phi}_j$ is the data obtained from j th element of the hidden layer, m determines the number of neurons used in the hidden layer, and n indicates the number of elements introduced into the input layer, f_i indicates the output data, w and b are the weight and bias, respectively, used for the training. Equation (1) denotes the summation function based on the training parameters. Equation (2) is used to calculate the hidden layer output after $\hat{\Phi}_j$ is defined. Collected data, following training, are used to understand how to categorize the knowledge from experience. To find network quality during the training, the validation dataset is used. If the performance is poor, the network must change those parameters dynamically to achieve precision. One of the most important design difficulties in ANN applications is determining the number of hidden nodes (HN). Under-fitting is more common when there are fewer HN. However, if HN are too numerous, the network will suffer from an over-fitting problem, following which it will only generate robust predictions during the training phase but will perform poorly during the testing phase [46].

2.2 Butterfly optimization algorithm

BOA [20] is a nature-inspired meta-heuristic algorithm

representing butterfly foraging and mating behavior. Each butterfly has its own distinct fragrance, which sets BOA apart from other meta-heuristics. As a function of the physical intensity of stimulation, the fragrance is created as follows:

$$f_i = cI^a, \quad (3)$$

where f_i denotes the perceived fragrance magnitude, c is the sensory modality, I is the stimulation intensity, and a is the power exponent depending on the degree of fragrance absorption. The global and local search phases are the two most essential phases in the algorithm. The following Eq. (4) is a mathematical model of the butterfly's global search movements:

$$x_i^{t+1} = x_i^t + (r^2 \times g_{\text{best}} - x_i^t) \times f_i, \quad (4)$$

where x_i^t is the i th butterfly's solution vector x_i in iteration number t . g_{best} is the current best solution identified among all the solutions in the current iteration. The i th butterfly's fragrance is represented by f_i , while r is a random number $[0,1]$. The following formulation can present the local search phase:

$$x_i^{t+1} = x_i^t + (r^2 \times x_i^k - x_i^t) \times f_i, \quad (5)$$

where x_j^t and x_i^k are j th and k th butterflies selected randomly from the solution space. The butterfly transforms into a local random walk if x_j^t and x_i^k belong to the same iteration. If not, the solution will become more diverse due to this random movement. In nature, butterflies can look for food and a mating partner on a global and local scale. To convert between the usual global search and the intense local search, a switch probability ρ is specified. The BOA produces a number in the range $[0,1]$ at random in each iteration, and this is compared with the switch probability ρ to determine whether to execute a global or local search.

2.3 Method statement

In this work, a computational intelligence approach based on BOA-ANN as a hybrid technique is used for damage prediction. Each butterfly (solution) in the proposed technique has three parts: connection weights between the input, hidden and output layer connection weights, and biases. The connections are represented by the network weights, which are real numbers in the range $[-1,1]$. To put it another way, each solution is represented by a vector of real numbers in the range $[-1,1]$. The number of elements in this vector may be estimated using the following formula:

$$\text{vector length} = (n \times m) + (2 \times m) + 1, \quad (6)$$

where n denotes the number of input features in the

dataset, and m is the number of nodes in the hidden layer. Classification Error Percentage (*CEP*) is used to evaluate the accuracy of classification problems as described in Eqs. (3) and (4). $\vec{O}_p = (O_{p1}, \dots, O_{pn})$ and $\vec{t}_p = (t_{p1}, \dots, t_{pn})$ where n is the number of ANN output units and O_{pi} and t_{pi} are predicted and target values of i th output unit. $\vec{P} = (P_1, \dots, P_k)$ is an input pattern in which k is the number of ANN inputs, and P is the number of patterns [47].

$$\Psi(\vec{P}) = \begin{cases} 1, & \text{if } \vec{O}_p \neq \vec{t}_p, \\ 0, & \text{otherwise,} \end{cases} \quad (7)$$

$$CEP = 100 \times \left(\sum_{p=1}^P \frac{\Psi(\vec{P})}{P} \right). \quad (8)$$

The Root Mean Squared Error (*RMSE*) is used as a fitness function to solve the approximation problem. In this study, all numerical studies are implemented in MATLAB R2017a. The following steps are programmed while using BOA-ANN.

Step 1: Data preparation and initialization of the number of populations and search agents.

Step 2: Creation of a population that is completely random.

Step 3: Retrieval of the selected feature and HN size, calculation and evaluation of the fitness values for each butterfly and assignment of the vector of parameters (biases and weights).

Step 4: Creation of a network and start of training using the provided training dataset.

Step 5: Calculation of the mean square error (*MSE*), simulation of the final network using validation data. Computation of each individual's fitness based on the validation *MSE*.

Step 6: Generation of the next population, and performance of the current optimal butterfly.

Step 7: Repeat of Steps 3 to 6 until the maximum generation is reached.

Step 8: Achievement of the final performance (classification accuracy and HN size), and use of the test data to simulate the optimal network.

3 Numerical simulations

A model-dependent vibration-based analysis requires an accurate numerical model prior to experiments. A commercial software, ABAQUS 16.4, is used to create the FEM of intact and damaged steel beam with boundary condition (Free-Free). The geometrical and mechanical properties are presented in Table 1. Figure 2(a) shows the finite element mesh of the steel beam having 350 continuum elements, and the locations of the damages (Fig. 2(b)) are represented by cracks of various depths which have been produced at two points along the beam's length, in the center; and on the right side. Table 2 shows the frequencies for intact beams based on numerical and experimental studies using a different number of elements. The torsional modes have been ignored for practical reasons. The three first mode shapes are presented in Fig. 3.

4 Results and discussion

In order to evaluate the BOA-ANN technique for crack depth prediction, two damage cases are explored. In the first case, the crack was produced across the middle width of the beam by gradually increasing the crack depth from 3 to 30 mm in 0.5 mm steps. In the second case, the crack was formed on the beam's right side by increasing the crack depth from 3 to 30 mm with a 0.5 mm step. BOA-ANN is trained considering two different numbers of neurons, which are 4 and 8. The power exponent α is taken between [0.1, 0.3], and the switch probability $\rho = 0.5$. To investigate the performance of BOA for ANN

Table 1 Geometrical and mechanical characteristics of beam mode

item	value
length, L (mm)	700
width, W (mm)	50
thickness, t (mm)	6
density, ρ (kg/m ³)	7850
Young's modulus, E (GPa)	210
Poisson's ratio, ν	0.3

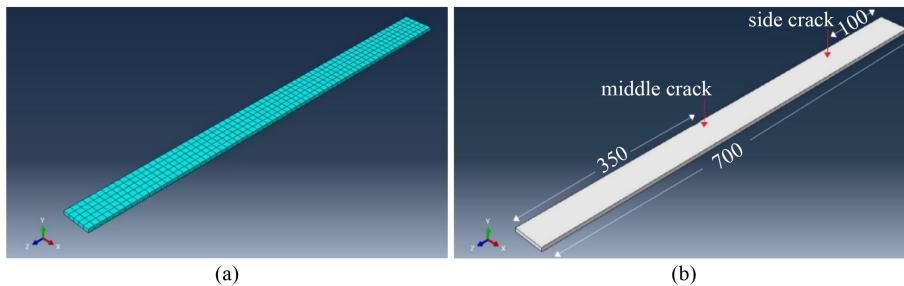
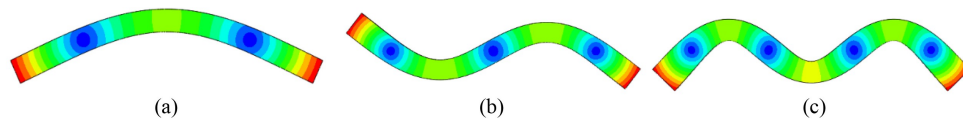


Fig. 2 (a) Finite element model and (b) considered beam model with considered damage location (mm).

Table 2 FEM and Measured Frequencies of the intact beam model

cases	element number				frequency		
	length	width	thickness	total	Model 1 (Hz)	Model 2 (Hz)	Model 3 (Hz)
Case 1	70	5	1	350	521.78	1394.2	2622.8
Case 2	140	10	1	1400	530.13	1416.4	2663.9
Case 3	175	13	2	4550	531.26	1419.4	2669.5
Case 4	700	50	6	210000	532.78	1423.5	2677.0
experimental	–	–	–	–	531.05	1420	2645.5

**Fig. 3** The first three mode shapes of the intact beam. (a) Model 1; (b) Model 2; (c) Model 3.

training, a comparative study is investigated with GA-ANN and PSO-ANN, and the selected number of generations and populations is 1000. In this study, the computer characteristics used are Intel Core TM i7 and 16 Go DDR4 3200 MHz. Four scenarios are considered for each side, as presented in Table 3.

4.1 Middle crack damage case

In this damage case, we apply BOA-ANN to predict middle crack depth. The regression study of BOA-ANN compared with PSO-ANN and GA-ANN of each hidden layer size is presented in Fig. 4. The obtained results are summarized in Table 4. The given results for each test demonstrate that BOA-ANN has the best performance study compared to PSO and GA. The regression is extremely close to 1, and the hidden layer size of $n = 8$ gives the best performance case. The maximum error of the the most results is within the range of 0.2 mm when the predicted and desired results are compared. The results also indicate that PSO and GA can predict the crack depth but with lower performance than BOA. The error range is more significant and requires a large number of generations and populations, up to 1000, which requires more time for calculation. The best computational time can be found in BOA-ANN between 76 and 88 s, compared with a significant difference in GA-ANN. However, the number of training points needs to be increased as well, so that accuracy can be further improved by choosing more extensive networks. Figure 5 shows a summary of the obtained results.

4.2 Side crack damage case

We apply BOA-ANN to predict the side crack depth in this damage case. Figure 6 shows the BOA-ANN regression study compared with PSO-ANN and GA-ANN for each hidden layer size. Table 5 summarizes the obtained results. The given results for each test

Table 3 Considered cracks depths scenarios

damage cases	crack depth (mm)
middle crack	6, 13.5, 21, 29.5
side crack	3.5, 11, 18.5, 29

Table 4 Predicted crack depth for middle crack damage case using ANN trained by BOA-PSO-GA

n	real crack depth (mm)	predicted crack depth (mm)	error in predicted results (%)	computational time (s)
4	6	BOA: 6.2022	3.37	76.0815
		PSO: 6.2888	4.81	145.1284
		GA: 6.3621	6.04	1923.1515
	13.5	BOA: 13.4271	0.54	78.1111
		PSO: 13.2867	1.58	148.2450
		GA: 13.9275	3.17	1992.7564
	21	BOA: 21.0050	0.02	76.0105
		PSO: 21.1000	0.48	145.1212
		GA: 21.4322	2.06	1899.1122
8	29.5	BOA: 29.5312	0.11	80.0021
		PSO: 29.4912	0.03	140.2121
		GA: 29.1112	1.32	1920.2000
	6	BOA: 5.8710	2.15	88.8415
		PSO: 5.8520	2.47	162.3422
		GA: 5.5110	8.15	2127.2667
	13.5	BOA: 13.3726	0.94	81.8498
		PSO: 13.1229	2.79	141.3353
		GA: 13.9912	3.64	2008.3222
	21	BOA: 21.0919	0.44	83.1111
		PSO: 21.3000	1.43	149.9874
		GA: 20.3211	3.23	1992.9911
	29.5	BOA: 29.4955	0.02	84.2221
		PSO: 29.1911	1.05	141.1019
		GA: 28.5212	3.32	2083.0199

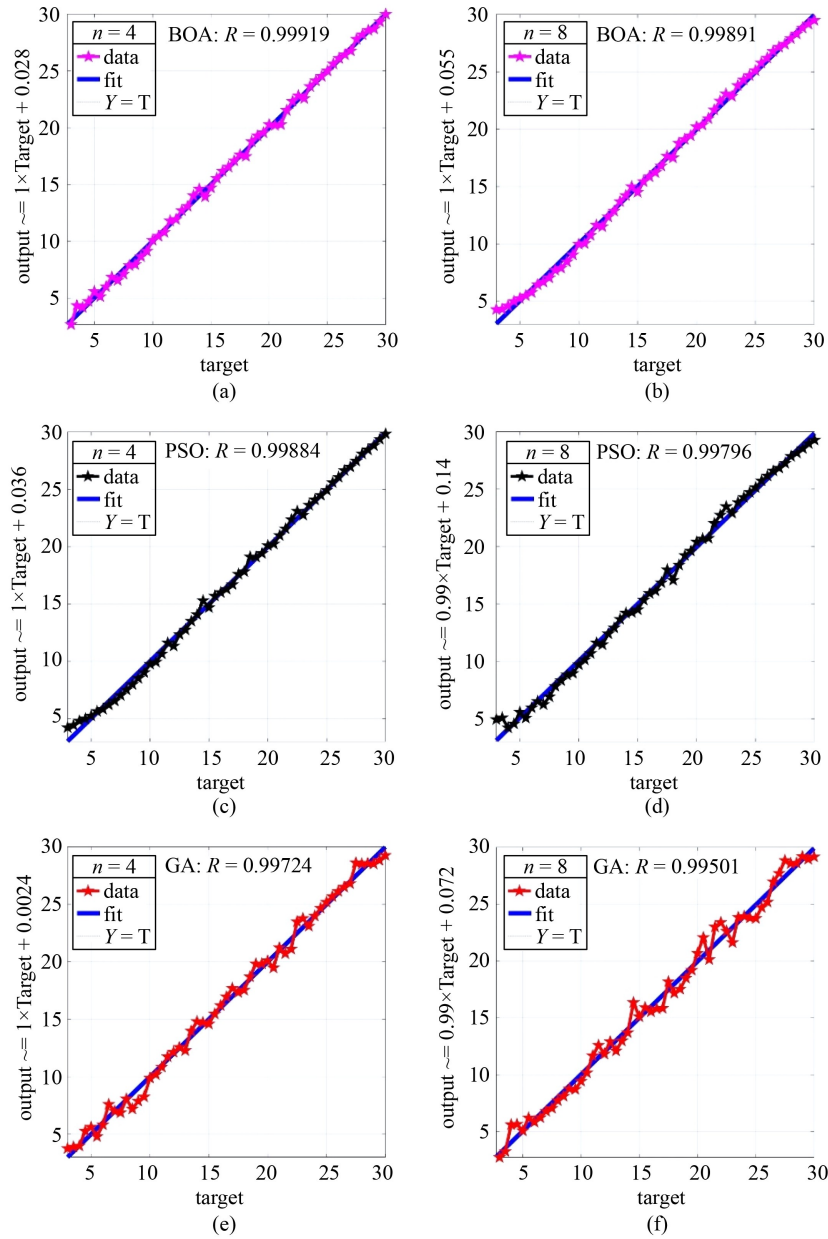


Fig. 4 Regression using different numbers of hidden layer sizes for middle crack damage case. BOA with (a) $n = 4$ and (b) $n = 8$; PSO with (c) $n = 4$ and (d) $n = 8$; GA with (e) $n = 4$ and (f) $n = 8$.

demonstrate that the regression is extremely close to 1 and that the hidden layer size of $n = 8$ provides the best performance study. Nevertheless, BOA requires fewer iterations and less computational time. The maximum error is less than 0.3 mm for BOA when the predicted and desired results are compared. The obtained results also indicate that by applying various hidden layer sizes, ANN enhanced by BOA can more reliably predict the crack depth for this damage case than PSO and GA. However, GA requiring more computational time and less accuracy. The best computational time can be found in BOA-ANN between 74 and 87 s, compared with a significant difference in GA-ANN. The MSE error decreases with increase in number of training points. Increase in the

number of training points also further improves accuracy by using more extensive networks. Figure 7 shows a summary of the obtained results.

5 Experimental validations

Using a particular impact hammer to activate the structural component and accelerometers to calculate device acceleration and experimental dynamic testing were carried out on a free-free beam model with mechanical characteristics mentioned in Table 1. The dynamic analysis of the beam model was conducted utilizing the LAN-XI TYPE 3050-Brüel & Kjaer data

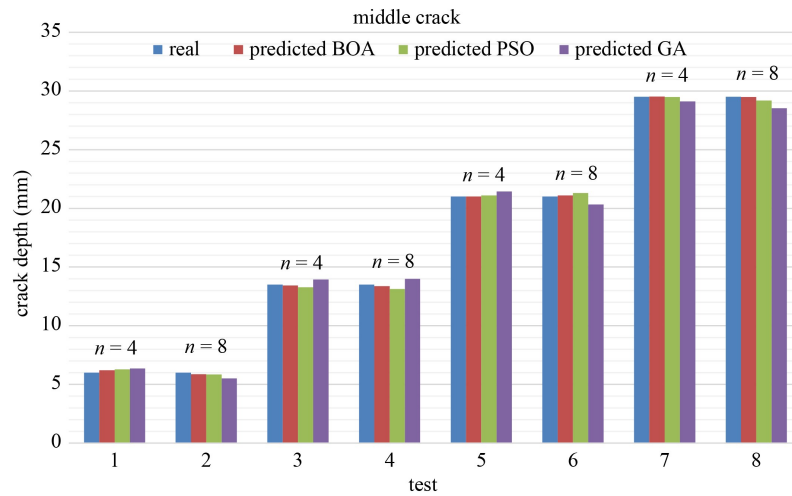


Fig. 5 Real and predicted crack depth by changing the hidden layer size for middle crack damage case.

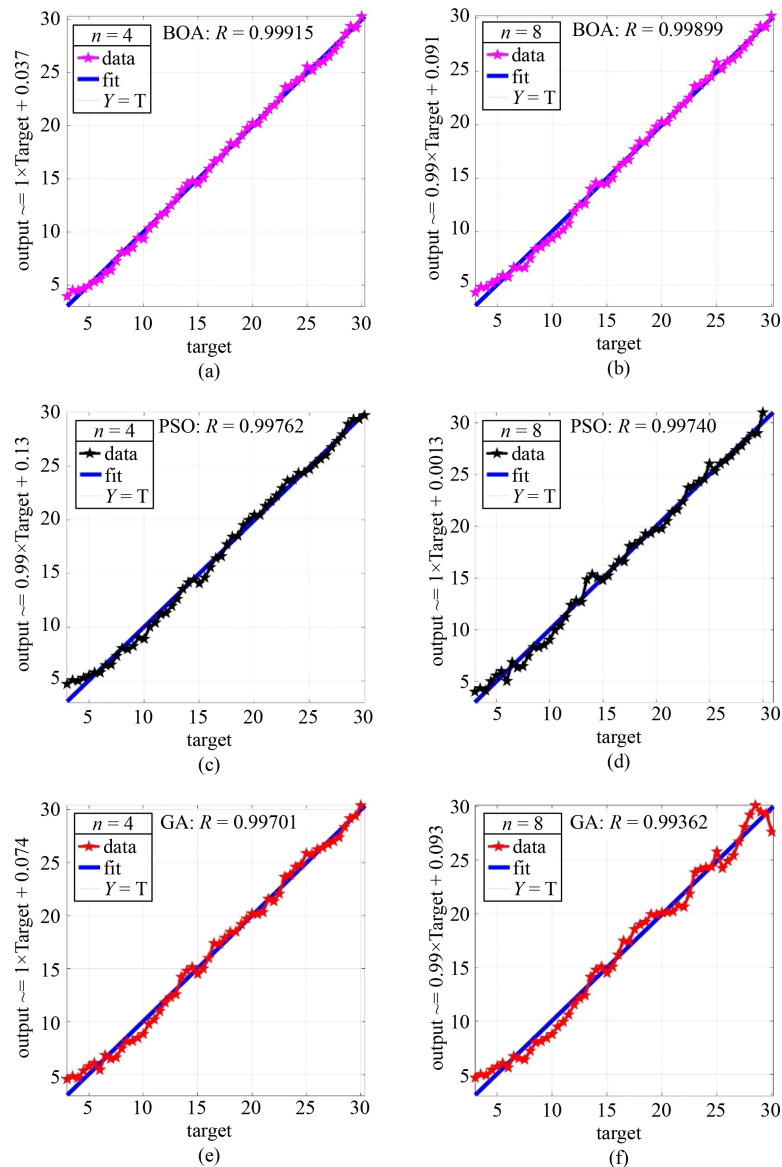


Fig. 6 Regression using a different number of hidden layer sizes for side crack damage case. BOA with (a) $n = 4$ and (b) $n = 8$; PSO with (c) $n = 4$ and (d) $n = 8$; GA with (e) $n = 4$ and (f) $n = 8$.

acquisition system to evaluate the experimental vibration findings via frequency domain measurement expressed by Frequency Response Function (FRF). The piezoelectric

Table 5 Predicted crack depth for side crack damage case using ANN trained by BOA-PSO-GA

n	real crack depth (mm)	predicted crack depth (mm)	error in predicted results (%)	computational time (s)
4	3.5	BOA: 3.7922	8.35	74.0215
		PSO: 3.8188	9.11	141.1114
		GA: 3.9121	11.77	1883.1215
	11	BOA: 10.9011	0.90	76.2211
		PSO: 10.5327	4.25	148.6660
		GA: 10.1222	7.98	1922.6784
	18.5	BOA: 18.5848	0.46	76.0100
		PSO: 18.6811	0.98	148.0102
		GA: 18.7848	1.54	2002.1211
	29	BOA: 29.1012	0.35	77.0001
		PSO: 29.2912	1.00	152.1111
		GA: 29.2800	0.97	2093.0000
8	3.5	BOA: 3.7520	7.20	87.1422
		PSO: 3.6112	3.18	159.1123
		GA: 3.8523	10.07	2032.0432
	11	BOA: 10.9011	0.90	86.8888
		PSO: 10.7111	2.63	140.3553
		GA: 10.2888	6.47	2099.9992
	18.5	BOA: 18.7999	1.62	84.7681
		PSO: 18.9360	2.36	149.1074
		GA: 19.0221	2.82	2032.1927
	29	BOA: 29.1911	0.66	84.2423
		PSO: 29.4215	1.45	141.1010
		GA: 27.7211	4.41	2011.1192

accelerometer and the impact hammer were connected to the data collecting system via the input channels, respectively, as shown in Fig. 8, whereas a piezoelectric accelerometer (Type 4508) was inserted at regular 150 mm intervals on four points. A measuring system capable of extracting frequency values by converting signals in the frequency domain using the Fast Fourier Transform (FFT) technique and Pulse software was used. A set of 10 hits for each accelerometer location was performed, and the average value was obtained. Next, frequency values were measured. A mechanical saw was used to make specimen cracks depths, as shown in Fig. 8. The scenarios of each crack depth are presented in Table 6.

FRF with measurements of vibration recorded by the accelerometer for damaged beam models by a middle crack with 5 and 25 mm depth and side crack with 10 and 20 mm depth are presented in Figs. 9–12, respectively. In Table 7, the experimental frequency values for damaged beams by middle and side cracks.

5.1 Results and discussion

In this section, BOA-ANN is trained using the experimental frequencies dataset given in Table 7 in order to predict the crack depth for the middle and side crack damage cases. The parameters for BOA-ANN are the power exponent a taken between 0.1 and 0.3, the switch probability $p = 0.5$, and $n = 8$ for hidden layer size. In Fig. 13, BOA-ANN regressions compared to those for PSO-ANN and GA-ANN are presented. The results are summarized in Table 8. The results for each test show that the regression is extremely near to 1 and the maximum error is found to be less than 0.2 mm for BOA when the predicted and desired results are compared with those for PSO and GA, for which the error range reaches up to 2.5 mm with a number of generations and populations reaching 1000. The results indicate that applying ANN enhanced by BOA can predict the crack

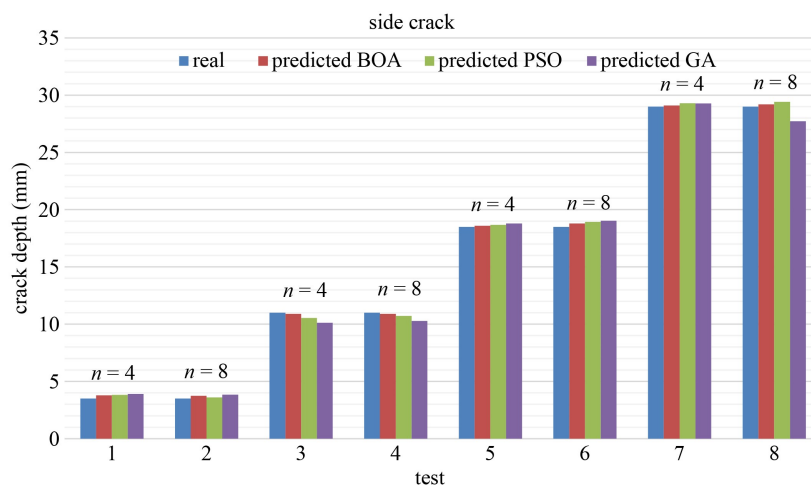


Fig. 7 Real and predicted crack depth by changing the hidden layer size for side crack damage case.

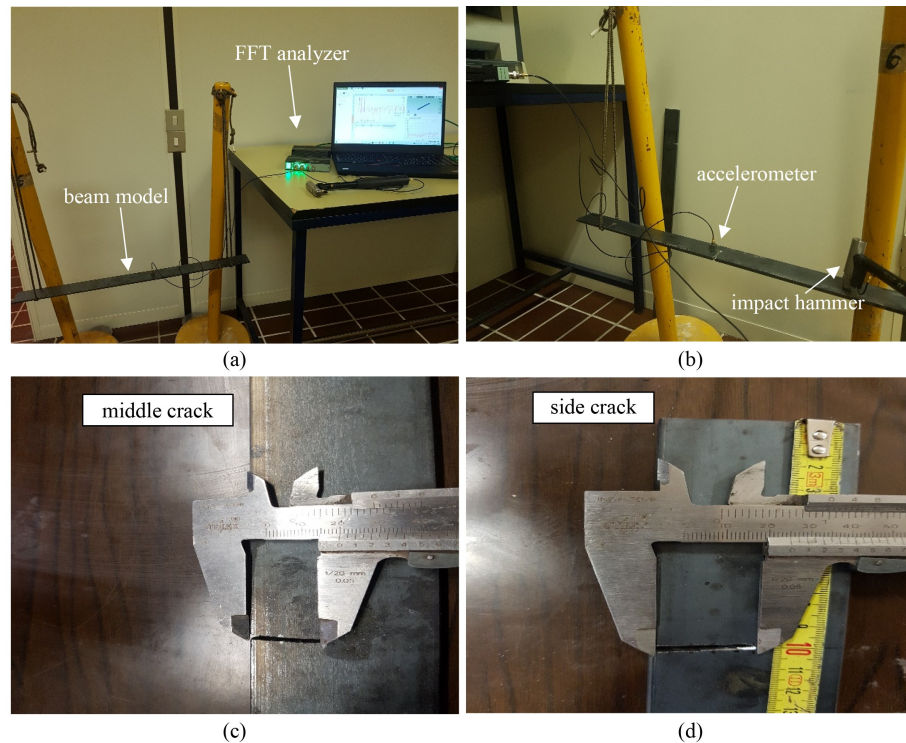


Fig. 8 Setup of cracked beam modal analysis. (a) Experimental setup; (b) impact and accelerometer position; (c) middle crack specimens; (d) side crack specimens.

Table 6 Considered cracks depths for experimental study

damage cases	crack depth (mm)
middle & side crack	5
	10
	15
	20
	25
	30

depth for both damage cases with the best accuracy.

Figures 14–15 show a summary of the results.

6 Conclusions

This study developed a hybrid approach based on BOA-ANN for damage prediction using finite element models as a tool to extract data. ANN is used as the basic architecture of the prediction model. Next, BOA is used to improve ANN parameters for better training. The approach is based on frequencies as input data and cracks depth as output data. Experimental modal analysis was used to acquire data for BOA-ANN, and a comparison is made with GA and PSO to test the accuracy of the presented approach. The predicted results appear to be very close to the expected output. The most significant error was 0.3 mm for BOA-ANN, whereas it was larger

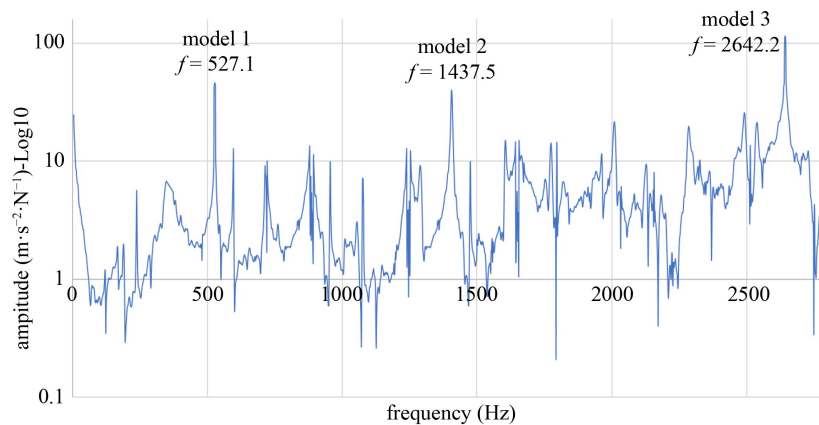


Fig. 9 FRF diagrams for middle crack damaged beam with 5 mm depth.

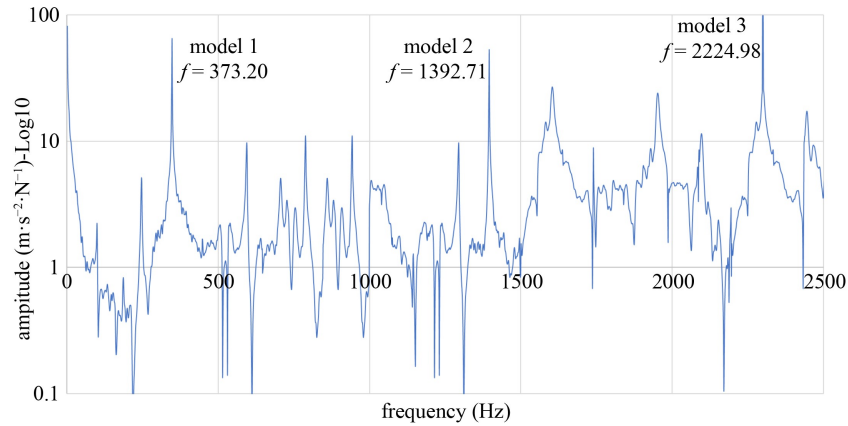


Fig. 10 FRF diagrams for middle crack damaged beam with 25 mm depth.

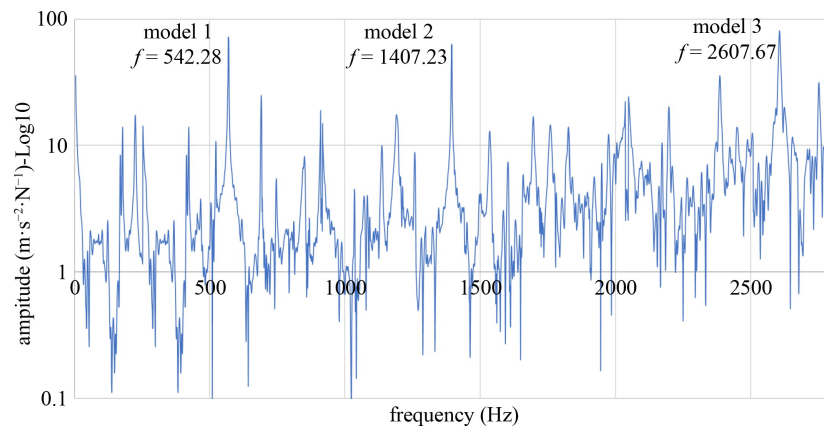


Fig. 11 FRF diagrams for side crack damaged beam with 10 mm depth.

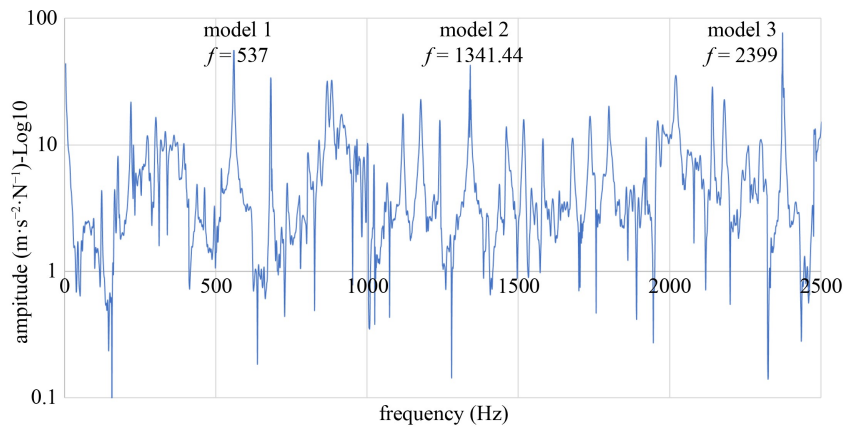


Fig. 12 FRF diagrams for side crack damaged beam with 20 mm depth.

Table 7 Experimental frequency values for damaged beam by middle and side crack

crack depth (mm)	middle crack (Hz)			side crack (Hz)		
	model 1	model 2	model 3	model 1	model 2	model 3
5	527	1437.20	2642.12	544.23	1420.22	2642.89
10	508.80	1431.28	2566.80	542.28	1407.23	2607.67
15	474.13	1428.10	2478	540.12	1393.65	2512.44
20	414.56	1411.80	2357.10	537	1341.44	2399
25	373.20	1392.71	2224.98	531.08	1240.65	2231.11
30	344.13	1380.22	2083.11	519	1111.31	2011.76

Table 8 Predicted crack depth for middle and side crack damage case using experimental data and ANN trained by BOA-PSO-GA

damaged case	<i>n</i>	real crack depth (mm)	predicted crack depth (mm)	error in predicted results (%)
middle crack	8	5	BOA: 5.0699	1.40
			PSO: 5.1890	3.78
			GA: 5.3777	7.55
		10	BOA: 9.9065	0.94
			PSO: 9.8911	1.09
			GA: 9.7221	2.78
		15	BOA: 15.0604	0.40
			PSO: 14.9200	0.53
			GA: 14.9001	0.67
		20	BOA: 20.0640	0.32
			PSO: 20.9132	4.57
			GA: 21.0921	5.46
		25	BOA: 25.2289	0.92
			PSO: 26.2763	5.11
			GA: 26.7321	6.93
		30	BOA: 29.9715	0.10
			PSO: 30.3938	1.31
			GA: 32.5864	8.62
side crack	8	5	BOA: 4.9915	0.17
			PSO: 5.1511	3.02
			GA: 5.3887	7.77
		10	BOA: 9.2565	7.43
			PSO: 9.5341	4.66
			GA: 9.0891	9.11
		15	BOA: 15.0933	0.62
			PSO: 14.8220	1.19
			GA: 14.5231	3.18
		20	BOA: 20.1110	0.56
			PSO: 20.7132	3.57
			GA: 20.2921	1.46
		25	BOA: 25.2289	0.92
			PSO: 25.3763	1.51
			GA: 25.7101	2.84
		30	BOA: 29.9719	0.09
			PSO: 30.3915	1.31
			GA: 31.9004	6.33

for PSO-ANN and GA-ANN and these also required more computational time. The BOA-ANN accuracy confirms that it provides a reliable way of obtaining the necessary results and, as a result, identifying the crack with the lowest number of errors. The training set can be increased even more to improve the accuracy of the results. The proposed approach will be enhanced in future

work based on new input parameters and more complex structures.

Acknowledgements This experimental research was supported by research funds provided by Università Politecnica Delle Marche. The authors would like to express their gratitude to all the technicians and students who collaborated to develop the experimental research.

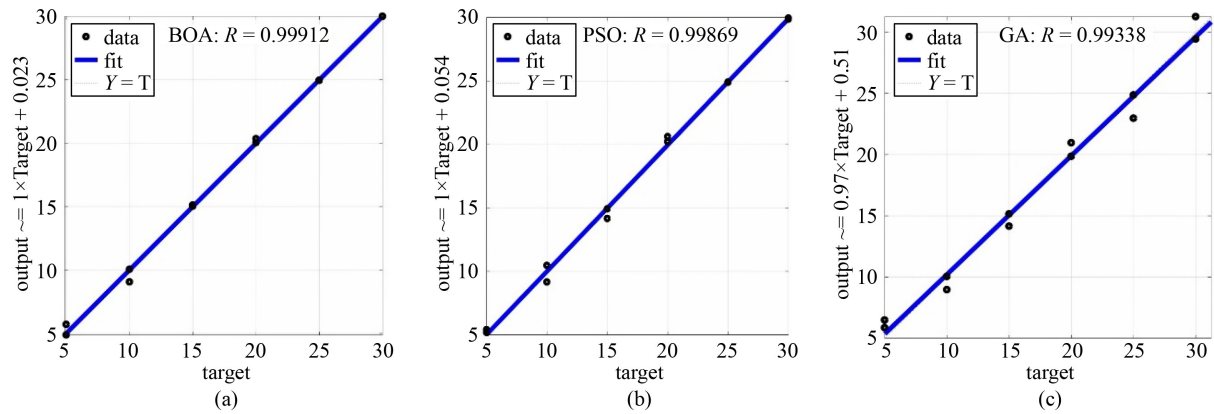


Fig. 13 Regression study for ANN trained with (a) BOA; (b) PSO; (c) GA.

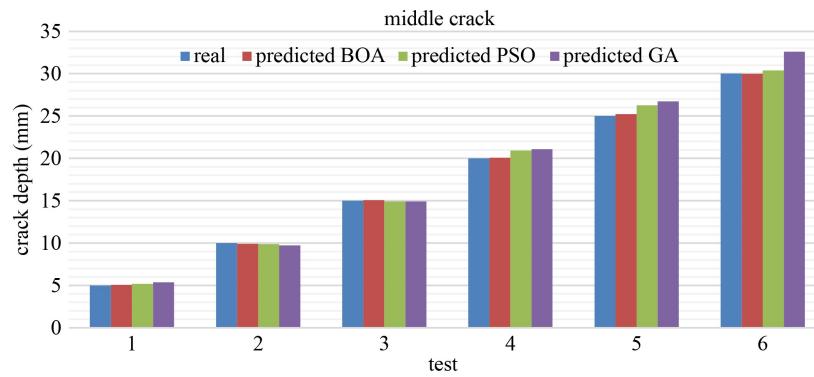


Fig. 14 Experiment middle crack prediction using ANN trained by BOA-PSO-GA.

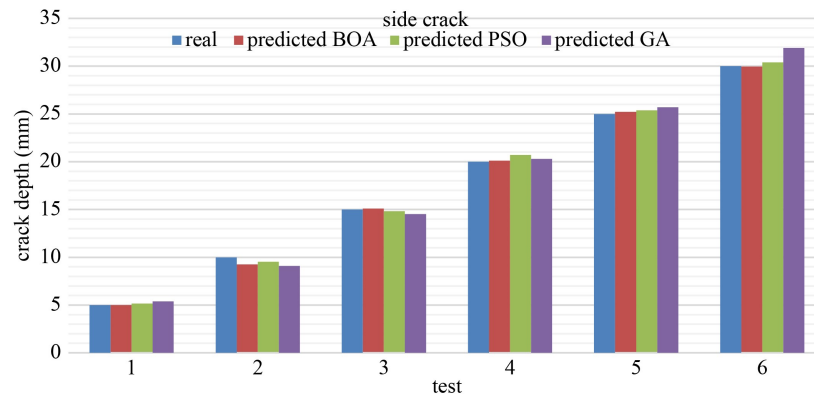


Fig. 15 Experiment side crack prediction using ANN trained by BOA-PSO-GA.

References

- Magagnini E, Khatir S. Effect of damage by notches in the vibration response of homogeneous and heterogeneous beam models. *Lecture Notes in Civil Engineering*, 2021, 148: 187–197
- Capozucca R, Magagnini E. Analysis of cracked RC beams under vibration. *Journal of Physics: Conference Series*, 2017, 842(1): 012076
- Kumar P, Siddiqui A, Ghadi A, Tony D, Rhenius S, Rane S. Damage detection in beams using vibration analysis and artificial neural network. In: *2021 4th Biennial International Conference on Nascent Technologies in Engineering (ICNTE)*. Chengdu: IEEE, 2021, 1–5
- Seguini M, Khatir S, Boutchicha D, Nedjar D, Wahab M A. Crack prediction in pipeline using ANN-PSO based on numerical and experimental modal analysis. *Smart Structures and Systems*, 2021, 27: 507–523
- Khatir S, Boutchicha D, Le Thanh C, Tran-Ngoc H, Nguyen T N, Abdel-Wahab M. Improved ANN technique combined with Jaya algorithm for crack identification in plates using XIGA and experimental analysis. *Theoretical and Applied Fracture Mechanics*, 2020, 107: 102554

6. Nourani B, Salmasi F, Ghorbani M A. Modeling and estimating the uplift force of gravity dams using finite element and artificial neural network whale optimization algorithm methods. *Amirkabir Journal of Civil Engineering*, 2020, 52(7): 393–396
7. Mehrjoo M, Khaji N, Moharrami H, Bahreininejad A. Damage detection of truss bridge joints using artificial neural networks. *Expert Systems with Applications*, 2008, 35(3): 1122–1131
8. Yeung W T, Smith J W. Damage detection in bridges using neural networks for pattern recognition of vibration signatures. *Engineering Structures*, 2005, 27(5): 685–698
9. Khatir S, Wahab M A, Tiachacht S, Le Thanh C, Capozucca R, Magagnini E, Benaissa B. Damage identification in steel plate using FRF and inverse analysis. *Fracture and Structural Integrity*, 2021, 15(58): 416–433
10. Maity D, Saha A. Damage assessment in structure from changes in static parameter using neural networks. *Sadhana*, 2004, 29(3): 315–327
11. Cunha E, Caetano E. Experimental modal analysis of civil engineering structures. *Sound and Vibration*, 2006, 40: 12–20
12. Padil K H, Bakhary N, Muyideen A, Li J, Hao H. Non-probabilistic method to consider uncertainties in frequency response function for vibration-based damage detection using artificial neural network. *Journal of Sound and Vibration*, 2020, 467: 115069
13. Khiem N T, Lien T V. Multi-crack detection for beam by the natural frequencies. *Journal of Sound and Vibration*, 2004, 273(1–2): 175–184
14. Lee J J, Lee J W, Yi J H, Yun C B, Jung H Y. Neural networks-based damage detection for bridges considering errors in baseline finite element models. *Journal of Sound and Vibration*, 2005, 280(3–5): 555–578
15. Anitescu C, Atroshchenko E, Alajlan N, Rabczuk T. Artificial neural network methods for the solution of second order boundary value problems. *Computers, Materials & Continua*, 2019, 59(1): 345–359
16. Samaniego E, Anitescu C, Goswami S, Nguyen-Thanh V M, Guo H, Hamdia K, Zhuang X, Rabczuk T. An energy approach to the solution of partial differential equations in computational mechanics via machine learning: Concepts, implementation and applications. *Computer Methods in Applied Mechanics and Engineering*, 2020, 362: 112790
17. Zhuang X, Guo H, Alajlan N, Zhu H, Rabczuk T. Deep autoencoder based energy method for the bending, vibration, and buckling analysis of Kirchhoff plates with transfer learning. *European Journal of Mechanics. A, Solids*, 2021, 87: 104225
18. Guo H, Zhuang X, Rabczuk T. A deep collocation method for the bending analysis of Kirchhoff plate. 2021, arXiv:2102.02617
19. Nguyen-Thanh V M, Anitescu C, Alajlan N, Rabczuk T, Zhuang X. Parametric deep energy approach for elasticity accounting for strain gradient effects. *Computer Methods in Applied Mechanics and Engineering*, 2021, 386: 114096
20. Nanthakumar S S, Lahmer T, Zhuang X, Zi G, Rabczuk T. Detection of material interfaces using a regularized level set method in piezoelectric structures. *Inverse Problems in Science and Engineering*, 2016, 24(1): 153–176
21. Arora S, Singh S. Butterfly optimization algorithm: A novel approach for global optimization. *Soft Computing*, 2019, 23(3): 715–734
22. Arora S, Singh S. An improved butterfly optimization algorithm with chaos. *Journal of Intelligent & Fuzzy Systems*, 2017, 32(1): 1079–1088
23. Arora S, Singh S. An effective hybrid butterfly optimization algorithm with artificial bee colony for numerical optimization. *International Journal of Interactive Multimedia and Artificial Intelligence*, 2017, 4(4): 14–21
24. Faravelli L, Materazzi F, Rarina M. Genetic algorithms for structural identification. *Proceedings of ICOSAR*, 2005, 5: 3115–3121
25. Casciati S. Stiffness identification and damage localization via differential evolution algorithms. *Structural Control and Health Monitoring*, 2008, 15(3): 436–449
26. Khatir A, Tehami M, Khatir S, Abdel Wahab M. Multiple damage detection and localization in beam-like and complex structures using co-ordinate modal assurance criterion combined with firefly and genetic algorithms. *Journal of Vibroengineering*, 2016, 18(8): 5063–5073
27. Samir K, Idir B, Serra R, Brahim B, Aicha A. Genetic algorithm based objective functions comparative study for damage detection and localization in beam structures. *Journal of Physics: Conference Series*, 2015, 628(1): 012035
28. Horibe T, Watanabe K. Crack identification of plates using genetic algorithm. *JSME International Journal Series A Solid Mechanics and Material Engineering*, 2006, 49(3): 403–410
29. Lai X, Zhang M. An efficient ensemble of GA and PSO for real function optimization. In: *Proceedings of the 2009 2nd IEEE International Conference on Computer Science and Information Technology*. Beijing: IEEE, 2009, 651–655
30. Khatir A, Tehami M, Khatir S, Wahab M A. Damage detection and localization on thin plates using vibration analysis. *Research in Veterinary Science*, 2016, 106: 107–111
31. Zenzen R, Belaidi I, Khatir S, Wahab M A. A damage identification technique for beam-like and truss structures based on FRF and Bat Algorithm. *Mecanical Reports*, 2018, 346(12): 1253–1266
32. Ghannadi P, Kourehli S S. Structural damage detection based on MAC flexibility and frequency using moth-flame algorithm. *Structural Engineering and Mechanics*, 2019, 70(6): 649–659
33. Moezi S A, Zakeri E, Zare A, Nedaei M. On the application of modified cuckoo optimization algorithm to the crack detection problem of cantilever Euler–Bernoulli beam. *Computers & Structures*, 2015, 157: 42–50
34. Kim J T, Stubbs N. Crack detection in beam type structures using frequency data. *Journal of Sound and Vibration*, 2003, 259(1): 145–160
35. Huang M, Cheng S, Zhang H, Gul M, Lu H. Structural damage identification under temperature variations based on PSO–CS hybrid algorithm. *International Journal of Structural Stability and Dynamics*, 2019, 19(11): 1950139
36. Baghmisheh M V, Peimani M, Sadeghi M H, Etefagh M M, Tabrizi A F. A hybrid particle swarm–Nelder–Mead optimization method for crack detection in cantilever beams. *Applied Soft Computing*, 2012, 12(8): 2217–2226

37. Vakil-Baghmisheh M T, Peimani M, Sadeghi M H, Ettetfagh M M. Crack detection in beam-like structures using genetic algorithms. *Applied Soft Computing*, 2008, 8(2): 1150–1160
38. Dehuri S, Cho S B. A hybrid genetic based functional link artificial neural network with a statistical comparison of classifiers over multiple datasets. *Neural Computing & Applications*, 2010, 19(2): 317–328
39. Awan S M, Aslam M, Khan Z A, Saeed H. An efficient model based on artificial bee colony optimization algorithm with Neural Networks for electric load forecasting. *Neural Computing & Applications*, 2014, 25(7–8): 1967–1978
40. Mirjalili S Z, Saremi S, Mirjalili S M. Designing evolutionary feedforward neural networks using social spider optimization algorithm. *Neural Computing & Applications*, 2015, 26(8): 1919–1928
41. Chen J F, Do Q H, Hsieh H N. Training artificial neural networks by a hybrid PSO-CS algorithm. *Algorithms*, 2015, 8(2): 292–308
42. Rukhaiyar S, Alam M N, Samadhiya N K. A PSO-ANN hybrid model for predicting factor of safety of slope. *International Journal of Geotechnical Engineering*, 2018, 12(6): 556–566
43. Shahrouzi M, Sabzi A H. Damage detection of truss structures by hybrid immune system and teaching–learning-based optimization. *Asian Journal of Civil Engineering*, 2018, 19(7): 811–825
44. Tran-Ngoc H, He L, Reynders E, Khatir S, Le-Xuan T, De Roeck G, Bui-Tien T, Wahab M A. An efficient approach to model updating for a multispan railway bridge using orthogonal diagonalization combined with improved particle swarm optimization. *Journal of Sound and Vibration*, 2020, 476: 115315
45. Chatterjee S, Sarkar S, Hore S, Dey N, Ashour A S, Balas V E. Particle swarm optimization trained neural network for structural failure prediction of multistoried RC buildings. *Neural Computing & Applications*, 2017, 28(8): 2005–2016
46. Ahmad F, Mat-Isa N A, Hussain Z, Boudville R, Osman M K. Genetic Algorithm-Artificial Neural Network (GA-ANN) hybrid intelligence for cancer diagnosis. In: 2010 2nd International Conference on Computational Intelligence, Communication Systems and Networks. Liverpool: IEEE, 2010, 78–83
47. Yaghini M, Khoshraftar M M, Fallahi M. A hybrid algorithm for artificial neural network training. *Engineering Applications of Artificial Intelligence*, 2013, 26(1): 293–301